Theoretical study of resonant ultrashort-pulse propagation in semiconductors

A. Knorr,* R. Binder, M. Lindberg, and S. W. Koch
Optical Sciences Center, University of Arizona, Tucson, Arizona 85721
and Physics Department, University of Arizona, Tucson, Arizona 85721
(Received 21 April 1992; revised manuscript received 23 July 1992)

Femtosecond-pulse propagation in resonantly excited semiconductors is investigated by numerically solving the semiconductor Maxwell-Bloch equations for plane waves. For excitation at the exciton resonance, it is shown that the pulse absorption exhibits a strongly nonlinear dependence on the input pulse area. Very long propagation distances for strong pulses are observed, but even when all dephasing processes have been neglected, no lossless propagation (self-induced transparency) was found. The influence of the electron-hole many-body effects, nonequilibrium carrier relaxation, and optical dephasing on the pulse-propagation dynamics is studied. The exchange interaction in the electron-hole plasma is shown to support large propagation distances. For excitation of the continuum states, the dependence of the absorption on the intensity of the input pulse is reduced due to the rapid carrier relaxation into quasiequilibrium distributions.

PACS number(s): 42.50.Md

I. INTRODUCTION

The development of a substantial variety of femtosecond laser sources make it possible to study coherent optical effects in semiconductor media. Examples include the excitonic Stark effect [1–11], photon echo [12–15], ultrafast adiabatic following [16], and more. Concerning the propagation dynamics of ultrafast light pulses under resonant excitation conditions, however, only few theoretical investigations have been performed until now [17].

Generally, it is known that the propagation of high-power pulses in matter alters the linear absorption law of Lambert and Beer. For the case of atomic systems there are two situations in which the pulse propagation has been particularly well studied. The first one is the case of coherent propagation of optical pulses through an ensemble of absorbing atomic systems. The most important result for this situation is summarized in terms of the area theorem of McCall and Hahn [18,19]. The area theorem describes phenomena such as lossless propagation in ensembles of inhomogeneously broadened two-level systems and break up of propagating pulses [18–20]. A well-known effect observed in atomic systems is the phenomenon of self-induced transparency (SIT) for pulses that are shorter than the characteristic dephasing time of the matter system. SIT describes the special property of sufficiently strong optical pulses to travel anomalously long distances in resonant absorbers [18,19].

The second well-studied regime is realized when the light-matter interaction time is long compared to characteristic decay times of the material. In this case incoherent effects are dominant and the system is described by the Frantz-Nodvik formula, which includes saturation phenomena of the optical transition [21]. Both the area theorem and the Frantz-Nodvik formula are valid for two-level systems coupled to each other only through the external electromagnetic field.

In contrast to the two-level dynamics, the generated charge carriers in semiconductors are not only coupled by the external optical field, but they also interact via the Coulomb interaction. This coupling of different one-particle states leads to additional terms in the optical Bloch equations, altering the polarization of the medium and thus the source term that acts on the propagating electromagnetic field. Furthermore, the dephasing time in highly excited semiconductors is often of the order of ~ 100 fs [22–28], i.e., of the order of the duration of the shortest light pulses that are experimentally generated to excite the system.

In this paper we study how electron-hole many-body interactions, carrier relaxation, and optical dephasing influence the propagation of femtosecond pulses in semiconductors. To study this problem, we numerically investigate the semiconductor Maxwell-Bloch equations, i.e., the semiconductor Bloch equations coupled to the wave equation for the slowly varying envelope of a propagating light field. Before we present our numerical results in Sec. III we summarize in Sec. II the basic equations and relevant parameters.

II. BASIC EQUATIONS

In this section we present the basic equations that govern the interaction between a propagating light pulse and a semiconductor medium. The light-matter interaction is treated semiclassically by solving the coupled set of Maxwell-Bloch equations for the field. We consider a laser pulse with a carrier frequency ω_L and apply the slowly varying envelope representation for the electric field $E(z,t)$ and the polarization $P(z,t)$:

$$E(t,z)=\tfrac{1}{2}\tilde{E}(z,t)e^{i(\omega_L t-k_L z)}+\text{c.c.}\ ,$$
$$P(z,t)=\tilde{P}(z,t)e^{i(\omega_L t-k_L z)}+\text{c.c.} \tag{1}$$

Here we restrict ourselves to the propagation of plane waves traveling in the z direction. The propagation con-

stant k_L and the carrier frequency ω_L are related by the linear dispersion relation of the medium. Using the slowly varying envelope approximation and introducing a coordinate frame (ξ,η) traveling at the group velocity v_g of the light pulse, we find the reduced wave equation

$$\frac{\partial\tilde{E}(\xi,\eta)}{\partial\xi}=-i\mu_0\frac{\omega_L^2}{k_L}\tilde{P}(\xi,\eta)\ ,\quad \xi=z\ ,\quad \eta=t-\frac{z}{v_g}\ . \tag{2}$$

The group velocity v_g is given by the linear dispersive properties of the semiconductor. The resonant electronic polarization $P(\xi,\eta)$ has to be computed from the semiconductor Bloch equations. These equations were derived by several authors [5–8] and have been shown to be a good approximation in the investigation of local properties of semiconductors excited by electromagnetic fields. The coherent part of the equations results from a Hartree-Fock approximation in the equations of motion. Additionally, a realistic description of highly excited semiconductors has to take into account screening of the Coulomb potential and dephasing of the polarization.

The semiconductor Bloch equations can be written as

$$\left[\frac{\partial}{\partial\eta}+i[\omega_L-\omega_k(\xi,\eta)]+\frac{1}{T_2}\right]\tilde{P}_k(\xi,\eta)$$
$$=-i[1-f_k^e(\xi,\eta)-f_k^h(\xi,\eta)]\tilde{\Omega}_k(\xi,\eta)\ ,$$
$$\frac{\partial f_k^e(\xi,\eta)}{\partial\eta}=i[\tilde{\Omega}_k^*(\xi,\eta)\tilde{P}_k(\xi,\eta)-\text{c.c.}]$$
$$-\frac{1}{T_1}[f_k^e(\xi,\eta)-f_{k0}^e(\xi,\eta)]\ , \tag{3}$$
$$\frac{\partial f_k^h(\xi,\eta)}{\partial\eta}=i[\tilde{\Omega}_k^*(\xi,\eta)\tilde{P}_k(\xi,\eta)-\text{c.c.}]$$
$$-\frac{1}{T_1}[f_k^h(\xi,\eta)-f_{k0}^h(\xi,\eta)]\ ,$$

where $f_k^{e/h}$ are the carrier distribution functions for electrons and holes, respectively, and P_k is the polarization for a given one-particle momentum state. The total polarization is obtained by summing the contributions of all momentum states, including the two different spin states:

$$\tilde{P}(\xi,\eta)=2\sum_k d_{cv}\tilde{P}_k(\xi,\eta)\ , \tag{4}$$

and the renormalized energy ω_k and the local field Ω_k are given by

$$\hbar\omega_k=\frac{\hbar^2k^2}{2m_r}+\hbar\omega_g-\sum_q V_{|k-q|}(f_q^e+f_q^h)$$
$$+\sum_q(V_{|k-q|}-V_{|k-q|}^0)\ , \tag{5}$$
$$\hbar\tilde{\Omega}_k=\tfrac{1}{2}\tilde{E}d_{cv}+\sum_q V_{|k-q|}\tilde{P}_q\ . \tag{6}$$

Furthermore, d_{cv} is the interband dipole matrix element, $\hbar\omega_g$ is the semiconductor band-gap energy, T_1 is the carrier relaxation time, and T_2 is the polarization decay time, respectively. Equations (3)–(6) are valid for semiconductors that are spatially homogeneous on a scale of several exciton Bohr radii. The spatial dependence in the propagation direction (coordinate $z=\xi$) is used as a parameter for the pulse propagation described by Eq. (2).

The dephasing of the system is modeled by a constant dephasing rate $1/T_2$. The phase relaxation time T_2 is to be expected on the femtosecond time scale [22–28]. The scattering of the electron-hole population is included in the relaxation-time approximation [28]. The screening of the Coulomb potential is described in the quasistatic approximation

$$V_k=\frac{e^2}{\epsilon_b\epsilon_0|k|^2}\left[1+\frac{\kappa^2}{|k|^2+\kappa^2\left[\dfrac{\hbar|k|^2}{2m_r\omega_{\text{pl}}}\right]^2}\right]^{-1} \tag{7}$$

with the inverse screening length

$$\kappa^2=\frac{e^2}{\epsilon_b\epsilon_0\hbar^2\pi^2}\left[m_e\int_0^\infty dk\, f_k^e+m_h\int_0^\infty dk\, f_k^h\right] \tag{8}$$

and the plasma frequency

$$\omega_{\text{pl}}^2=\frac{e^2}{\epsilon_b\epsilon_0 m_r}n(\xi,\eta)\ . \tag{9}$$

Here n denotes the total carrier density of electrons $n=2\sum_k f_k^e=2\sum_k f_k^h$, $\epsilon_0\epsilon_b$ is the dielectric constant in the medium, and m_r is the reduced electron-hole mass. The unscreened Coulomb potential V_k^0 is defined by taking the limit $\kappa\to 0$ in (7). The terms $\sum_q V_{k-q}P_qf_k$, $\sum_q V_{k-q}f_qP_k$, and $\sum_q V_{k-q}P_qP_k^*$ are often referred to as "exchange contributions," and we use this terminology also in the present paper. For the case of a vanishing interaction potential V_k the semiconductor Bloch equations (3) reduce to the two-level Bloch equations.

In the case of the semiconductor the Coulomb potential couples different k states of the medium. One could therefore expect that complicated interference effects might destroy such coherent effects as Rabi oscillations and therefore the possibility of SIT. However it was shown in [16] that semiconductors excited at the exciton resonance show Rabi-like oscillations in the time dependence of the carrier density. Moreover, the density was found to show almost twice as many Rabi flops as one would expect for a corresponding two-level system. This behavior is explained by the effective amplification of the electric field E due to the Coulomb interaction term in the effective Rabi energy (6). In the next section we show how the many-body effects influence the propagation of ultrashort light pulses and discuss the differences to the propagation of light in two-level systems.

III. RESULTS AND DISCUSSION

A. Coherent pulse propagation

In order to gain some insight into pulse propagation in semiconductors under idealized conditions we neglect in this section all relaxation processes and screening effects. This allows comparison with the solitonlike propagation known from the two-level dynamics. From Eqs. (2) and (3) we find a propagation equation for the intensity of the field

$$\frac{\partial}{\partial \xi}\left|\frac{d_{cv}\tilde{E}(\xi,\eta)}{2\hbar}\right|^2=\sigma\frac{\partial}{\partial \eta}\sum_k f_k^e(\xi,\eta)\ , \tag{10}$$

where σ is defined by

$$\sigma=-\frac{|d_{cv}|^2\mu_0\omega_L^2}{\hbar k_L}\ . \tag{11}$$

After integrating Eq. (10) with respect to time we find that the spatial dependence of the pulse energy $W=(c\epsilon_0/2)\int|E(t)|^2dt$ is proportional to the density at the time after the pulse:

$$\frac{\partial}{\partial \xi}W(\xi)\sim\sum_k f_k^e(\xi,\eta=\infty)\ . \tag{12}$$

Note that Eqs. (10)–(12) are valid for two-level systems as well as for semiconductor materials. According to Eq. (12) the possibility of lossless propagation is given for pulse areas for which the density is returned to zero after the pulse, so that the density exhibits complete Rabi flops. Then the pulse intensity is not changed while propagating [Eq. (12)].

Such an ideal case is realized if a sech-shaped pulse of an area of 2π travels through an ideal two-level medium [18]. This pulse returns the rotating dipoles exactly to their initial state, so that lossless propagation is possible. Until now we could not find any pulse shape that satisfies such conditions in semiconductor media. Numerical investigations predict that a finite amount of total polarization and charge carriers are remaining in the medium after the pulse [16].

For the numerical treatment the sample length is discretized into N slices. Beginning with the first slice the semiconductor Bloch equations are solved using a fourth-order Runga-Kutta method in the time domain for the initial conditions $P_k(\xi,\eta=-\infty)=0$, $f_k^e(\xi,\eta=-\infty)=0$, and $f_k^h(\xi,\eta=-\infty)=0$. The Coulomb potential is integrated over the angle between k and q corresponding to [29]. To calculate the optical field the wave equation (2) is solved in the first slice of the sample by a Runge-Kutta method of second order in the spatial domain. The calculated electric field resulting from the first slice serves as an initial field for the second slice while all distribution functions and polarizations are again initially zero in the time domain. This method is repeated to propagate the optical field through the whole sample. The number of points used in the time domain was typically 2000, the k space is resolved by approximately 100–150 points, and the number N of slices over a propagation distance of $\alpha z=1$ is about 50–100. The propagation distance is measured in small signal absorption length α^{-1}, so that $z\alpha=1$ corresponds to the propagation distance after which the area of a low intensity pulse is reduced to $1/e$ of its original value.

To investigate the propagation of a pulse of an area of 2π we solved the system of coupled partial integro-differential equations [(2) and (3)] for the case of excitation by a sech-shaped pulse of a full width at half maximum (FWHM) of 100 fs. The laser frequency is chosen to excite the exciton resonance. If the generated excitons would behave like particles that can be described in terms of two-level systems, the sech-shaped pulse would travel without disturbance [18].

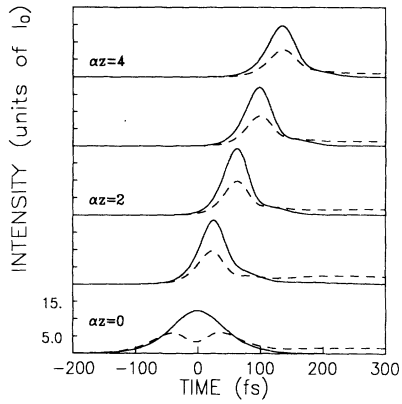

FIG. 1. Intensity (solid line) and density (dashed line) profiles for an initially 2π area sech-shaped light pulse at different positions in the semiconductor sample for the case of coherent propagation. This specific pulse shape would travel shape invariant in an ensemble of two-level systems $I_0=(10^{-4}\epsilon_0 c\hbar^2 fs^2)/(2d_{cv}^2)$.

We choose material parameters representative of the case of bulk CdSe: $m_e=0.125m_0$, $m_h=0.431m_0$, and the exciton Rydberg energy $E_{\rm exc}=16$ meV.

Figure 1 shows the computed pulse intensity (solid lines) and generated carrier density (dashed lines) at different positions in the sample. It can be seen from Fig. 1 that, in contrast to the two-level dynamics, the initial 2π pulse develops a shoulder and becomes shorter during the first part of the propagation. In the first slice of the sample, we confirm the result of Ref. [16] that the number of Rabi flops is nearly doubled compared to the same excitation conditions for a two-level system (Fig. 1, dashed line below). However, due to the remaining density in the system after the pulse, the energy of the electromagnetic field is slowly absorbed during its propagation. This can be seen from Fig. 1 by comparing the initial intensity profile and the profile after the propagation. Due to this absorption the effective Rabi frequency is gradually reduced so that the second Rabi flop cannot be maintained during the propagation through the sample.

In the case of a two-level system, a 2π pulse would create one Rabi flop following the shape of the pulse [18]. The doubling of Rabi flops in the semiconductor, which causes an oscillating temporal structure of the source terms in (10), leads to peak amplification and temporal compression of the field. To gain some analytical insight into the problem of coherent pulse propagation in a semiconductor, we show in our Appendix that SIT analogous to that in a two-level system cannot occur.

B. Incoherent propagation of pulses exciting the exciton resonance

The discussion in Sec. III A neglects dephasing processes in order to allow comparison of the results with the solitonlike propagation in atomic media, where dephasing times are often on the order of several nanoseconds. On the other hand, it is known that de-

phasing of the polarization and screening of the Coulomb potential are of significant importance for highly excited semiconductors. The phase relaxation times are often as short as ~ 100 fs.

Ultrashort laser pulses can have FWHM of ten to a few hundred femtoseconds. Therefore, under realistic circumstances one has to expect that the carrier relaxation and characteristic dephasing times T_1, T_2 are on the order of the pulse duration itself. To study this realistic situation we include optical dephasing, carrier scattering, and screening into the semiconductor Bloch equations as described in Sec. I, Eqs. (3)–(9).

We investigate again the propagation of light pulses with a FWHM of 100 fs, including finite relaxation times of $T_1 = 100$ fs, $T_2 = 100$ fs. The excitation is chosen to be at the exciton resonance. Sech-shaped pulses were found to be approximate solutions of the steady-state round trip equation of passively mode-locked lasers [30]. For this choice of the input pulse shape and input parameters we expect our results to be a reasonable approximation for experimentally relevant situations.

We depict in Fig. 2 the spatial development of the pulse intensity (solid line) of a 2π input pulse versus time. Additionally, the temporal profile of a light pulses of low intensity (here chosen to have an initial area of 0.1π) is shown as a dashed line. The comparison reveals that pulses of lower intensity are absorbed rapidly, whereas the 2π pulse suffers only a minor reduction of its peak intensity over several Lambert-Beer absorption lengths. The origin of this behavior can be traced back to the phase-space filling process in semiconductors and was already found in [17]. The phase-space filling effect is comparable to the saturation of the upper level in two-level systems. Schematically, the behavior can be understood such that the temporally first part of the pulse generates carriers and is partially absorbed, so that the second part is able to pass the sample without strong absorption. Figure 2 shows the pulse is gradually delayed during the propagation due to the described asymmetric absorption in time. In contrast to the case of coherent propagation (Fig. 1), no pulse compression can be observed. This is expected because the temporal change of the carrier density due to relaxation processes occurs on the same time scale as the pulse duration. Therefore, pulse-induced transient oscillations relax during the characteristic time in which they are generated. Consequently, peak amplification and compression of the pulse are not observed in the incoherent regime for the chosen parameters.

In Fig. 3 we compare the temporal development of the carrier density for the incoherent case (short-dashed line) and the coherent case (long-dashed line) to show that the Rabi-like oscillations are not pronounced enough to lead to pulse compression if the relaxation times are on the order of the pulse duration itself. Due to the finite phase relaxation time the generated density is larger than in the coherent case because the linewidth of the electron-hole transitions is broadened.

To investigate the origin of the pulse absorption we show in Fig. 4 the distribution function f_k^e of the electrons at different time delays (d) with respect to the peak intensity of the exciting pulse. If the absorption of the pulse energy occurs purely due to the generation of excitons the depicted distribution function would follow roughly the slope of the $1s$ exciton wave function. However, from Fig. 4 it can be seen that the excitation is moved further into the continuum states than the slope of the $1s$ exciton wave function. This was already discussed for far-off-resonant excitation in Ref. [11]. For resonant excitation with high pulse energies the maximum of the distribution function (time delay $d = 0$) is at much higher k values than the half width of the $1s$ exciton wave function. This effect is due to many-body effects like band-gap renormalization and amplification of the effective Rabi frequency. Therefore, the absorption of the propagating light pulse is not only determined simply by the generation of excitons but by more general many-body electron-hole effects. Furthermore, comparing the band-

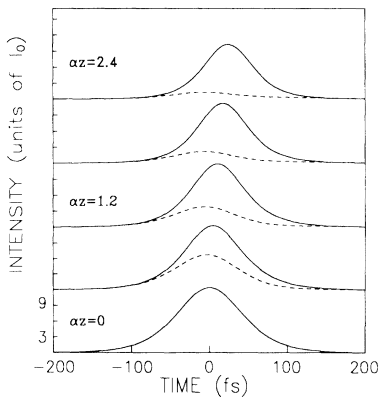

FIG. 2. Intensity profiles vs time at different positions in the semiconductor sample. Relaxation times and pulse duration are chosen to be 100 fs. The solid line shows the intensity of a pulse with an initial area of 2π. The dashed line shows the intensity of a 0.1π pulse. The distance between the curves is 0.6 Lambert-Beer absorption lengths.

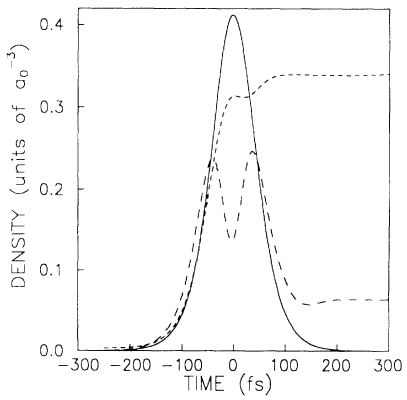

FIG. 3. Light-induced density vs time for the coherent case (long-dashed line) and the incoherent case (short-dashed line). The intensity profile of the incident pulse is shown as a solid line.

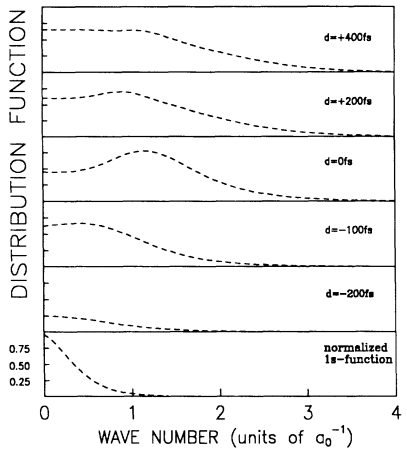

FIG. 4. Electron distribution function f_k^e for different delay times (d) inside the sample excited by a 2π pulse. The parameters are the same as in Fig. 2. The delay is measured with respect to the peak intensity of the pulse. The square of the normalized $1s$ exciton function is included for comparison. The normalization factor is given by $32\pi n(t)$, where $n(t)$ is the carrier density.

width of the light pulse (approximately 1 exciton Rydberg energy) with the bandwidth of the particle distribution (Fig. 4), it can be seen that the excitation energy is transferred into k regions that are not directly dipole coupled to the exciting electromagnetic field. This part of the excited states is lost for the reamplification process needed for true SIT-like propagation. Due to the band-gap renormalization the pulse interacts with the continuum of states even though the excitation frequency is originally at the exciton resonance.

To investigate the spectral energy distribution of the incident pulse we calculated the pulse spectrum, defined by

$$S(\omega-\omega_L)=\frac{1}{4\pi}\epsilon_0 c\left|\int_{-\infty}^{\infty} dt\,\tilde{E}(t)e^{i(\omega_L-\omega)t}\right|^2 . \qquad (13)$$

As can be seen from Fig. 5 the spectrum remains mainly

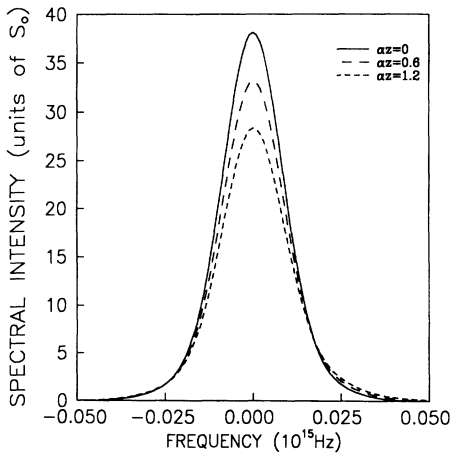

FIG. 5. Spectral intensity of a propagating 2π pulse at different positions in the semiconductor sample. Parameters are the same as in Fig. 2 [$S_0=1/(2\pi)10^4 I_0$].

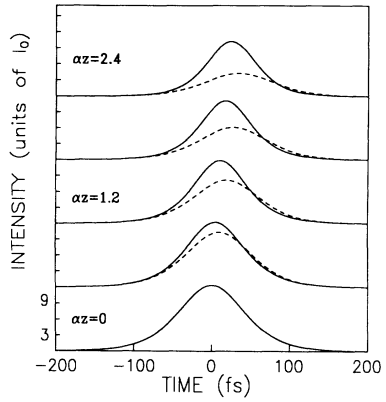

FIG. 6. Intensity profiles vs time at different positions in the semiconductor sample. Relaxation times and pulse duration are 100 fs. The solid line shows the intensity of a 2π pulse. The dashed line shows the solution with the same parameters but without exchange terms. The distance between the curves is 0.6 Lambert-Beer absorption lengths.

symmetric during its propagation. In general, an asymmetric density of states will result in an asymmetric pulse shape. In the present case, however, the density of states is essentially constant due to the interband Coulomb enhancement.

In order to understand the importance of the exchange terms in Eq. (3) for the anomalously long propagation distances in the high excitation case (Fig. 2, solid line) we solved Eqs. (2) and (3) without exchange contributions. As shown in Fig. 6 we find that for propagation in a system without exchange contributions the transmitted intensity (dashed line) is reduced by nearly a factor of 2 compared to the result that includes the exchange terms (solid line). The equations without exchange terms may yield carrier distributions that exceed unity and hence violate the Pauli principle. A consequence of this unphysical result is that the absorbing states can be populated by more carriers as if they would obey Fermi-Dirac statistics. This causes the electromagnetic field to lose more energy during its propagation as shown in Fig. 6. Hence the exchange terms obviously play an important role for the proper description of the resonant pulse propagation in semiconductors.

C. Incoherent propagation of pulses exciting above the band gap

Until now all calculations were made for the case where the optical frequency of the pulse is centered at the exciton resonance. If the light pulse excites the sample high above the band gap, the role of carrier relaxation is enhanced since the optically generated distribution functions deviate more strongly from Fermi functions. This deviation causes drastic changes in the pulse absorption since the influence of phase space filling on the pulse depletion is reduced. If the generated carriers leave the region of excitation fast enough the saturation of the transitions is suppressed and even a high intensity pulse nearly follows the linear absorption law of Lambert-Beer

To investigate this scenario the 2π pulse used in Sec.

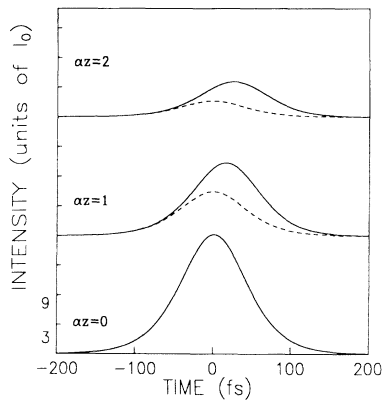

FIG. 7. Intensity profiles vs time at different positions in the semiconductor sample. Relaxation times and pulse duration are 100 fs. In contrast to Fig. 2 the excitation occurs highly above the band gap ($ka_0=4$). The solid line shows the intensity of a 2π pulse. The dashed line shows the intensity of a pulse with initially 0.1π pulse. All other parameters are the same as in Fig. 2. The distance between the curves is 1 Lambert-Beer absorption length.

III B is now assumed to excite the system at 16 exciton Rydberg energies above the band gap. The spectral width of the pulse is on the order of 1 Rydberg energy, thus the excitation is well above the band gap. We compare in Fig. 7 the propagation of a 0.1π and a 2π pulse. All other parameters are the same as in Sec. III B. As can be seen from Fig. 7 only relatively small differences occur between the absorption losses of the low (dashed line) and the high intensity pulse (solid line) in contrast to the case of excitation of the exciton resonance (Fig. 2). For excitation in the continuum both pulses are absorbed on the same length scale. The remaining difference in Fig. 7 is due to the fact that the relaxation of the carriers is on the order of the pulse duration, and not infinitely fast. In Fig. 8 we show the corresponding electron distribution function (dashed line) in comparison to the distribution function in the case in which the excitation occurs

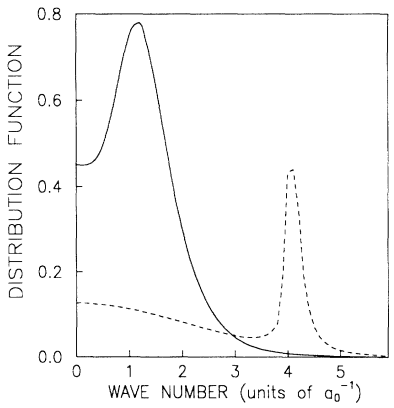

FIG. 8. Electron distribution function f_k^e for the case of excitation at the exciton resonance (solid line) and for excitation into the continuum (dashed line) after a propagation over one small signal absorption length.

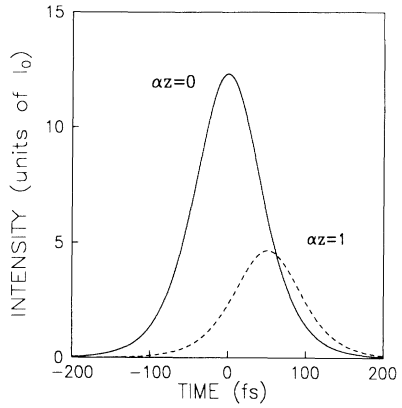

FIG. 9. Intensity profiles of 2π input pulse after the propagation over 1 Lambert-Beer absorption length in the semiconductor sample. In contrast to Fig. 6 the excitation occurs well below the band gap (eight exciton Rydberg energies). The solid line shows the intensity of a 2π input pulse. The dashed line shows the pulse intensity after the propagation. The solution without exchange terms shows no significant deviation.

in the exciton resonance (solid line) after the propagation of one small signal absorption length. It can be seen that in the case of excitation into the continuum states the intraband relaxation process transfers electrons out of the excitation region.

D. Incoherent propagation of pulses exciting below the band gap

For the excitation of a semiconductor well below the band gap it was shown in Ref. [11] that the exchange effects are of minor importance due to the smaller amount of generated carriers. Therefore it is expected that the exchange effects will not strongly influence the transmitted pulse energy compared to the case of resonant excitation where the occupation of the one-particle states is high (Fig. 6). To confirm this we show in Fig. 9 the results of our calculations for the temporal pulse profile if the carrier frequency of the pulse is centered 8 exciton energies below the semiconductor band gap. We could not find any significant difference between results with or without inclusion of the exchange terms. This is expected because the exchange effects are most relevant only when the one-particle states are highly occupied. A theory-experiment comparison of nonresonant pulse propagation in semiconductor waveguides can be found in Ref. [31].

IV. CONCLUSION

In conclusion, we present a theoretical study of resonant pulse propagation through semiconductor media. For excitation into the exciton resonance our numerical solutions of the semiconductor Maxwell-Bloch equations show that pulses with an area in excess of π propagate anomalously long distances, many times the length over which weak intensity pulses are completely absorbed. For the idealized case of vanishing dephasing and carrier relaxation we found pulse compression and Rabi flopping. Even though many of these features resemble the

phenomenon of self-induced transparency in atomic systems, true SIT in semiconductors is not obtained even under idealized conditions without dephasing and carrier scattering. For the excitation in the continuum we show that the input intensity dependence of the pulse propagation is reduced due to the intraband relaxation processes.

ACKNOWLEDGMENTS

We are sincerely grateful to E. M. Wright for valuable discussions. This work was supported by grants from NSF, ARO/AFOSR, NEDO, OCC and a grant for CPU time at the Pittsburgh Supercomputer Center. A.K. thanks the Studienstiftung des deutschen Volkes (Germany) for support.

APPENDIX

In this appendix we show that SIT exactly analogous to that in a two-level system cannot occur in a semiconductor. The proof is based on the approximation of a k-independent interaction matrix element. Since even in this case we find SIT to be impossible, we strongly believe SIT is all the more unlikely if a realistic Coulomb interaction would be considered. We will show that there can be no SIT in semiconductors analogous to the well-known two-level solutions with sech-pulse shapes. This pulse shape is to date the only known SIT solution in two-level systems. We therefore believe that it is not a very serious restriction when we investigate only semiconductor solutions analogous to those sech solutions.

The proof consists of two steps: First, we bring the semiconductor Maxwell-Bloch equations into a form that is identical to that of a two-level system. The only difference is the definition of an effective Rabi frequency. We then show that the regular sech solution for the effective Rabi frequency contradicts the analogous solution for the polarization and inversion functions.

A k-independent interaction potential allows the k sums in Eqs. (5) and (6) to be performed:

$$\sum_q V_{k-q} f_q = v \sum_q f_q = vF \ , \qquad \sum_q V_{k-q} \tilde{P}_q = v \sum_q \tilde{P}_q = v\tilde{P} \ , \tag{A1}$$

where the total polarization function P and the total density F for each spin degree of freedom have been introduced. Restricting ourselves to a soliton solution

$$\tilde{E} \to \tilde{E}(x) e^{i\delta z} \ , \quad \tilde{P}_k \to \tilde{P}_k(x) e^{i\delta z} \ , \quad f_k \to f_k(x) \ ,$$

where all functions depend on $x = t - z/v_g$, Eqs. (2) and (3) take the form

$$\left[\frac{\partial}{\partial x} + i(\omega_L - \omega_k) \right] \tilde{P}_k = -i(1-2f_k)\tilde{\Omega}_k \ , \tag{A2}$$

$$\frac{\partial}{\partial x} f_x = i(\tilde{\Omega}_k^* \tilde{P}_k - \text{c.c.}) \ , \tag{A3}$$

$$\tilde{P} = -i\frac{\beta}{\alpha}\frac{\partial}{\partial x}\tilde{\Omega} - \frac{\delta}{\alpha}\tilde{\Omega} \ , \tag{A4}$$

where we used the abbreviations

$$\hbar\omega_k = \frac{\hbar^2 k^2}{2m_r} + \hbar\omega_g - 2vF \ , \qquad \hbar\tilde{\Omega}_k = \tfrac{1}{2}\tilde{E}d_{cv} + vP \ , \quad \tilde{\Omega} = \frac{\tilde{E}d_{cv}}{\hbar} \ , \qquad \alpha = 2\mu_0 \frac{\omega_L^2 d_{cv}^2}{k_L \hbar} \ , \quad \beta = 1/v_g - 1/c \ . \tag{A5}$$

A constant of motion of these equations yields the relation

$$F = \frac{\beta}{2\alpha}|\tilde{\Omega}|^2 \ . \tag{A6}$$

Using Eqs. (A4) and (A5) we can now eliminate F and P in Eqs. (A2) and (A3) material. After the transformation

$$\tilde{P}_k \to \rho_k e^{i\Phi} \ , \quad \frac{\partial}{\partial x}\Phi = -2v\frac{\beta}{\alpha}|\tilde{\Omega}|^2 \ , \qquad \hbar\Delta_k = \hbar\omega_L - \hbar\omega_g - \frac{\hbar^2 k^2}{2m_r} \ , \tag{A7}$$

the Bloch equations assume a form exactly analogous to two-level systems:

$$\frac{\partial}{\partial x}\rho_k = -i\Delta_k \rho_k - i\tfrac{1}{2}(1-2f_k)\Omega_{\text{eff}} \ , \tag{A8}$$

$$\frac{\partial}{\partial x} f_k = i\tfrac{1}{2}(\Omega_{\text{eff}}^* \rho_k - \text{c.c.}) \ . \tag{A9}$$

Here the effective Rabi frequency

$$\Omega_{\text{eff}} = \left[\left[1 - 2v\frac{\delta}{\alpha} \right] \tilde{\Omega} - 2iv\frac{\beta}{\alpha}\frac{\partial}{\partial x}\tilde{\Omega} \right] e^{-i\Phi} \tag{A10}$$

has been introduced. The SIT solution requires Ω_{eff} to have a sech shape [18]

$$\Omega_{\text{eff}} = 2\gamma \, \text{sech}(x\gamma) \ . \tag{A11}$$

The corresponding solutions for the polarization and inversion functions are

$$\rho_k = \frac{-\Delta_k \gamma^{-1}}{1 + (\Delta_k \gamma^{-1})^2} \text{sech}(x\gamma) + \frac{i}{1 + (\Delta_k \gamma^{-1})^2} \text{sech}(x\gamma)\tanh(x\gamma) \ , \tag{A12}$$

$$f_k = \frac{1}{1 + (\Delta_k \gamma^{-1})^2} \text{sech}^2(x\gamma) \ . \tag{A13}$$

We can now formally perform the k summation and obtain

$$F = F_0 \text{sech}^2(\gamma x) \ , \tag{A14}$$

$$\tilde{P} = [\rho_0 \text{sech}(\gamma x) + iF_0 \tanh(\gamma x)\text{sech}(\gamma x)] e^{-i\Phi} \ , \tag{A15}$$

where

$$F_0=\sum_k \frac{1}{1+(\Delta_k\gamma^{-1})^2}\ ,\quad \rho_0=-\sum_k \frac{\Delta_k\gamma^{-1}}{1+(\Delta_k\gamma^{-1})^2}\ . \tag{A16}$$

The definition of Ω_{eff} [Eq. (A9)] and its solution Eq. (A10) yield

$$\left[\left[1-2v\frac{\delta}{\alpha}\right]\tilde{\Omega}-2iv\frac{\beta}{\alpha}\frac{\partial}{\partial x}\tilde{\Omega}\right]e^{-i\Phi}=2\gamma\ \mathrm{sech}(\gamma x)\ . \tag{A17}$$

We can eliminate here the derivative of $\tilde{\Omega}$ with the help of Eq. (A4), utilizing Eq. (A14), and obtain an equation for $\tilde{\Omega}$, which readily gives an expression for $|\tilde{\Omega}|^2$. On the other hand $|\tilde{\Omega}|^2$ is given by Eq. (A6), in which F is now the solution (A13). We finally can equate the two equations for $|\tilde{\Omega}|^2$:

$$\frac{2\alpha}{\beta}F_0\mathrm{sech}^2(\gamma x)=(-2v\rho_0+2\gamma)^2\mathrm{sech}^2(\gamma x)+4F_0v^2\tanh^2(\gamma x)\mathrm{sech}^2(\gamma x)\ . \tag{A18}$$

Hence only for $v=0$ the SIT solution is possible.

*Also at Institute for Optics and Quantum Electronics, Friedrich-Schiller-University, Max-Wien-Platz 1, O-6900 Jena, Germany.

[1] A. Mysyrowicz, D. Hulin, A. Antonetti, A. Migus, W. T. Masselink, and H. Morkoc, Phys. Rev. Lett. **56**, 2748 (1986).
[2] A. Von Lehmen, D. S. Chemla, G. E. Zinker, and G. P. Heritage, Opt. Lett. **11**, 609 (1986).
[3] D. Fröhlich, R. Wille, W. Schlapp, and G. Weimann, Phys. Rev. Lett. **59**, 1748 (1987).
[4] N. Peyghambarian, S. W. Koch, M. Lindberg, B. Fluegel, and M. Joffre, Phys. Rev. Lett. **62**, 1185 (1989).
[5] S. Schmitt-Rink, D. S. Chemla, and H. Haug, Phys. Rev. B **37**, 941 (1988).
[6] I. Balslev, R. Zimmermann, and A. Stahl, Phys. Rev. B **40**, 4095 (1989).
[7] W. Schäfer, *Festkörperprobleme (Advances in Solid State Physics),* edited by U. Roessler (Vieweg, Braunschweig, 1988), Vol. 28, p. 63.
[8] M. Lindberg and S. W. Koch, Phys. Rev. B **38**, 3342 (1988).
[9] R. Zimmerman and M. Hartmann, Phys. Status Solidi B **38**, 3342 (1988).
[10] C. Ell, J. F. Müller, K. ElSayd, and H. Haug, Phys. Rev. Lett. **62**, 304 (1989).
[11] R. Binder, S. W. Koch, M. Lindberg, W. Schäfer, and F. Jahnke, Phys. Rev. B **43**, 6520 (1991).
[12] P. C. Becker, H. L. Fragnito, C. H. Brito Cruz, R. L. Fork, J. E. Cunningham, J. E. Henry, and C. V. Shank, Phys. Rev. Lett. **61**, 1647 (1988).
[13] K. Leo, M. Wegener, J. Shah, D. S. Chemla, E. O. Göbel, T. C. Damen, S. Schmitt-Rink, and W. Schäfer, Phys. Rev. Lett. **65**, 1340 (1990).
[14] S. W. Koch, R. Binder, and M. Lindberg, in *Quantum Electronics Laser Science, 1991,* Vol. 11 of Technical Digest Series (Optical Society of America, Washington, DC, 1991), pp. 198 and 199.
[15] M. Lindberg, R. Binder, and S. W. Koch, Phys. Rev. A **45**, 1865 (1992).
[16] R. Binder, S. W. Koch, M. Lindberg, N. Peyghambarian, and W. Schäfer, Phys. Rev. Lett. **65**, 899 (1990).
[17] W. Schäfer and K. Henneberger, Phys. Status Solidi B **159**, 59 (1990).
[18] S. L. McCall and E. L. Hahn, Phys. Rev. Lett. **18**, 908 (1967).
[19] G. L. Lamb, Jr., Rev. Mod. Phys. **43**, 99 (1971).
[20] R. E. Slusher and H. M. Gibbs, Phys. Rev. A **5**, 1634 (1972).
[21] L. M. Frantz and J. S. Nodvik, J. Appl. Phys. **34**, 2346 (1963).
[22] For a review on various carrier scattering mechanisms in semiconductors see J. Shah, Solid-State Electron. **32**, 1051 (1989).
[23] W. H. Knox, D. S. Chemla, G. Livescu, J. E. Cunningham, and J. E. Henry, Phys. Rev. Lett. **61**, 1290 (1988).
[24] J. L. Oudar, A. Migus, D. Hulin, G. Grillon, J. Etchpare, and A. Antonetti, Phys. Rev. Lett. **53**, 384 (1984).
[25] C. V. Shank, R. C. Fork, R. Yen, J. Shah, B. I. Greene, A. C. Gossard, and C. Weisbuch, Solid State Commun. **47**, 981 (1983).
[26] H. Haug and D. B. Tran Thoai, Phys. Status Solidi B **98**, 581 (1980).
[27] C. Jacobini and L. Reggiani, Rev. Mod. Phys. **55**, 645 (1983).
[28] R. Binder, D. Scott, A. E. Paul, M. Lindberg, K. Henneberger, and S. W. Koch, Phys. Rev. B **45**, 1107 (1992).
[29] D. Dunn, J. Phys. C **10**, 2801 (1977).
[30] D. Kühlke, W. Rudolph, and B. Wilhelmi, IEEE J. Quantum Electron. **26**, 526 (1983).
[31] P. A. Harten, A. Knorr, J. P. Sokoloff, F. Brown de Colstoun, S. G. Lee, R. Jin, E. M. Wright, G. Khitrova, H. M. Gibbs, S. W. Koch, and N. Peyghambarian, Phys. Rev. Lett. **69**, 852 (1992).